Subgrid scale and backscatter model for magnetohydrodynamic turbulence based on closure theory: Theoretical formulation

Ye Zhou and Oleg Schilling
Lawrence Livermore National Laboratory, University of California, Livermore, California 94551

Sanjoy Ghosh
Emergent Information Technologies, Largo, Maryland 20774

(Received 4 June 2001; revised manuscript received 27 December 2001; published 27 August 2002)

The spectral eddy and backscatter viscosity and the spectral eddy and backscatter resistivity for incompressible, three-dimensional, isotropic, nonhelical magnetohydrodynamic (MHD) turbulence are constructed using the eddy-damped quasinormal Markovian statistical closure model developed by Pouquet, Frisch, and Léorat [J. Fluid Mech. **77**, 321 (1976)] in terms of primitive variables. The approach used is an extension of the methodology developed by Leslie and Quarini [J. Fluid Mech. **91**, 65 (1979)] for fluid turbulence to MHD turbulence. The eddy and backscatter viscosities and the eddy and backscatter resistivities are calculated numerically for assumed kinetic and magnetic energy spectra, $E_v(k)$ and $E_B(k)$, with a production subrange and a $k^{-5/3}$ inertial subrange for the two cases $r_A=1$ and $r_A=\frac{1}{2}$, where $r_A=E_v(k)/E_B(k)$ is the Alfvén ratio. It is shown that the effects of the unresolved subgrid scales on the resolved-scale velocity and magnetic field consist of an eddy damping and backscatter. The eddy viscosity and resistivity, and the backscatter viscosity and resistivity (the correlation function of the stochastic velocity and magnetic backscatter force) are shown to have a dependence on k/k_c, where k_c is the cutoff wave number, which is very similar to the dependence calculated in the pure (i.e., nonmagnetic) Navier-Stokes turbulence case. The eddy viscosity and resistivity, and the backscatter viscosity and resistivity numerically calculated here can be used to develop improved subgrid-scale parametrizations for spectral large-eddy simulations of homogenous MHD turbulence.

DOI: 10.1103/PhysRevE.66.026309 PACS number(s): 47.65.+a, 47.27.−i, 47.10.+g, 52.30.Cv

I. INTRODUCTION

Large-eddy simulation (LES) [1–3] is essentially the only practical method for computing the three-dimensional, time-dependent large scales of magnetohydrodynamic (MHD) flows [4,5] at large fluid and magnetic Reynolds numbers. As the subgrid scales are assumed to be universal, it is appropriate to model them using statistical methods. A subgrid scale and backscatter model that can satisfactorily reproduce the statistical effects of the small-scale dynamics on the resolved-scale dynamics is crucial for a successful LES. Although LES has been widely used in fluid turbulence simulations, it has not been widely applied in MHD turbulence because subgrid-scale modeling for MHD turbulence [6–8] is currently not well developed.

The eddy damping and the backscatter terms [9,10] in the resolved-scale velocity and magnetic field equations will be computed numerically here using the eddy-damped, quasinormal Markovian (EDQNM) closure model and *assumed forms* of the kinetic and magnetic energy spectra which have both a production subrange and a $k^{-5/3}$ power-law inertial subrange; the production and inertial subranges are generated by distinct mechanisms affecting the dynamics of the kinetic and magnetic energy. For the illustrative calculations presented here, the two Alfvén ratio cases $r_A=1$ and $r_A=\frac{1}{2}$ will be considered. The results of the present investigation are expected to be useful for the development of subgrid-scale models for spectral LES of large fluid and magnetic Reynolds number MHD turbulence encountered in space and astrophysical plasmas [13,14].

II. FILTERING AND THE MHD EQUATIONS

In this section, filtering in spectral space will be briefly reviewed, together with the equations for incompressible, three-dimensional, nonhelical MHD turbulence. The filtered MHD equations will also be presented.

A. Filtering

In LES, a filter $G(\mathbf{x},\mathbf{x}')$ [1,9] is introduced to partition the fields $f(\mathbf{x},t)$ into resolved-scale fields and subgrid-scale fields

$$\overline{f}(\mathbf{x},t)=\int G(\mathbf{x},\mathbf{x}')f(\mathbf{x}',t)d^3x', \tag{1}$$

$$f(\mathbf{x},t)'=f(\mathbf{x},t)-\overline{f}(\mathbf{x},t), \tag{2}$$

respectively. Here it is assumed that the filter is time independent and a scalar. This decomposition is performed for the velocity, magnetic field, and pressure in the MHD equations.

Most numerical simulations of MHD flows are performed for homogeneous turbulence, in which case the filtering operation can be written in spectral space as

$$\overline{f}(\mathbf{k},t)=G(\mathbf{k})f(\mathbf{k},t). \tag{3}$$

For homogeneous, isotropic turbulence, $G(\mathbf{k})=G(k)$, which will be used henceforth. The two filters most often used in subgrid-scale modeling and LES of fluid turbulence are the sharp cutoff filter and the Gaussian filter (the top-hat filter is similar to the Gaussian filter). With the cutoff wave number k_c, the sharp cutoff filter is

$$G(k)=\begin{cases}1 & \text{if } k<k_c\\ 0 & \text{if } k\geqslant k_c\end{cases} \tag{4}$$

which provides a sharp separation between resolved and unresolved scales (see Refs. [9], [15], [16]). This filter will be used in the present calculations.

B. The MHD equations

The standard MHD equations with zero mean fields and zero external forces are the velocity equation

$$\left(\frac{\partial}{\partial t}-\nu\nabla^2\right)\mathbf{v}=\mathbf{B}\cdot\nabla\mathbf{B}-\mathbf{v}\cdot\nabla\mathbf{v}-\nabla p \tag{5}$$

and the magnetic field equation

$$\left(\frac{\partial}{\partial t}-\xi\nabla^2\right)\mathbf{B}=\nabla\times(\mathbf{v}\times\mathbf{B}), \tag{6}$$

with the velocity $\mathbf{v}$ and the magnetic field $\mathbf{B}$ satisfying the solenoidality constraints

$$\nabla\cdot\mathbf{v}=\nabla\cdot\mathbf{B}=\mathbf{0}. \tag{7}$$

The constant kinematic viscosity and magnetic diffusivity are denoted by ν and ξ, respectively.

For homogeneous turbulence, the Fourier-transformed MHD equations in wave number space are

$$\left(\frac{\partial}{\partial t}+\nu k^2\right)v_i(\mathbf{k},t)=M_{ijk}(\mathbf{k})\sum^{\triangle}[v_j(\mathbf{p},t)v_k(\mathbf{q},t)-B_j(\mathbf{p},t)B_k(\mathbf{q},t)] \tag{8}$$

and

$$\left(\frac{\partial}{\partial t}+\xi k^2\right)B_i(\mathbf{k},t)=M^B_{ijk}(\mathbf{k})\sum^{\triangle}B_j(\mathbf{p},t)v_k(\mathbf{q},t), \tag{9}$$

where $\Sigma^{\triangle}$ represents the summation over $\mathbf{p}$ and $\mathbf{q}$ with the triadic restriction $\mathbf{k}=\mathbf{p}+\mathbf{q}$. The three-point interaction tensors are defined as

$$M_{ijk}(\mathbf{k})=-\frac{i}{2}[k_kP_{ij}(\mathbf{k})+k_jP_{ik}(\mathbf{k})], \tag{10}$$

$$M^B_{ijk}(\mathbf{k})=i\epsilon_{ilm}k_l\epsilon_{mjk}, \tag{11}$$

where ϵ_{ijk} is the unit antisymmetric tensor and the solenoidal projection tensor is $P_{ij}(\mathbf{k})=\delta_{ij}-k_ik_j/k^2$.

C. The filtered MHD equations

The filtered velocity and magnetic fields in wave number space are

$$\overline{v_i}(\mathbf{k},t)=G(k)v_i(\mathbf{k},t), \tag{12}$$

$$\overline{B_i}(\mathbf{k},t)=G(k)B_i(\mathbf{k},t), \tag{13}$$

respectively. The filtered velocity equation is

$$\left(\frac{\partial}{\partial t}+\nu k^2\right)\overline{v_i}(\mathbf{k},t)=M_{ijk}(\mathbf{k})\sum^{\triangle}G(k)[v_j(\mathbf{p},t)v_k(\mathbf{q},t)-B_j(\mathbf{p},t)B_k(\mathbf{q},t)] \tag{14}$$

and the filtered magnetic field equation is

$$\left(\frac{\partial}{\partial t}+\xi k^2\right)\overline{B_i}(\mathbf{k},t)=M^B_{ijk}(\mathbf{k})\sum^{\triangle}G(k)B_j(\mathbf{p},t)v_k(\mathbf{q},t). \tag{15}$$

III. EDDY DAMPING AND BACKSCATTER IN MHD TURBULENCE

A. The resolved-scale energy spectrum evolution equations

Accurate subgrid-scale modeling in MHD can be achieved using the second moment energy transfer equation [17–20]. Only the case of nonhelical, and statistically stationary MHD turbulence is considered here. Following Leslie and Quarini [9], the resolved-scale kinetic energy and magnetic energy spectrum are

$$\overline{E}_v(k,t)=\frac{k^2}{2}\int G(k)^2\langle v_i(\mathbf{k},t)v_i(-\mathbf{k},t)\rangle d\Omega_k, \tag{16}$$

$$\overline{E}_B(k,t)=\frac{k^2}{2}\int G(k)^2\langle B_i(\mathbf{k},t)B_i(-\mathbf{k},t)\rangle d\Omega_k, \tag{17}$$

respectively, where the integration is over the isotropic solid angle Ω_k.

In the EDQNM approximation, the resolved-scale kinetic energy and magnetic energy spectrum evolution equations are

$$\left(\frac{\partial}{\partial t}+2\nu k^2\right)\overline{E}_v(k,t)=\int\int_{\triangle}G(k)\,\theta_{kpq}(t)(T^{vv}_v+T^{vB}_v+T^{BB}_v)dp\,dq, \tag{18}$$

$$\left(\frac{\partial}{\partial t}+2\xi k^2\right)\overline{E}_B(k,t)=\int\int_{\triangle}G(k)\,\theta_{kpq}(t)(T^{vB}_B+T^{BB}_B)dp\,dq, \tag{19}$$

respectively, where [19,20]

$$T^{vv}_v(k,p,q,t)=\frac{k}{pq}b_{kpq}[k^2E_v(p,t)-p^2E_v(k,t)]E_v(q,t), \tag{20}$$

$$T^{vB}_v(k,p,q,t)=-\frac{kp}{q}c_{kpq}E_v(k,t)E_B(q,t), \tag{21}$$

$$T_v^{BB}(k,p,q,t)=\frac{k^3}{pq}c_{kpq}E_B(p,t)E_B(q,t), \tag{22}$$

$$T_B^{vB}(k,p,q,t)=\frac{k^5}{p^3q}c_{kpq}E_v(p,t)E_B(q,t) + \frac{k}{pq}h_{kpq}[k^2E_B(p,t)-p^2E_B(k,t)]E_v(q,t), \tag{23}$$

$$T_B^{BB}(k,p,q,t)=-\frac{k^3}{pq}c_{kpq}E_B(k,t)E_B(q,t). \tag{24}$$

The geometrical coefficients are

$$b_{kpq}=\frac{p}{k}(xy+z^3), \tag{25}$$

$$c_{kpq}=\frac{p}{k}z(1-y^2), \tag{26}$$

$$h_{kpq}=\frac{p}{k}(z+xy), \tag{27}$$

(x, y, and z are the cosines of the interior angles opposite the sides formed by **k**, **p**, and **q**, respectively), and the three-point correlation time scale is

$$\theta_{kpq}(t)=\frac{1}{\eta_k(t)+\eta_p(t)+\eta_q(t)}, \tag{28}$$

with eddy-damping rate

$$\eta_k(t)=(\nu+\xi)k^2+0.19\mathrm{Ko}^{3/2}\{k^3[E_v(k,t)+E_B(k,t)]\}^{1/2} + \sqrt{2/3}k\left[\int_0^k E_B(p,t)dp\right]^{1/2}, \tag{29}$$

where Ko is the Kolmogorov constant.

B. Formal expressions for the eddy damping and backscatter

The eddy viscosity and backscatter viscosity are given by

$$\nu_t(k|k_c;t)=\frac{1}{k^2}\int\int_\triangle G(k)\theta_{kpq}(t)\frac{kp}{q}[b_{kpq}E_v(q,t) + c_{kpq}E_B(q,t)]dp\,dq, \tag{30}$$

$$\nu_b(k|k_c;t)=\frac{1}{2k^2\overline{E_v}(k,t)}\int\int_\triangle G(k)\theta_{kpq}(t) \times\frac{k^3}{pq}\left\{b_{kpq}E_v(p,t)E_v(q,t) + c_{kpq}\frac{p^2}{k^2}E_v(k,t)E_B(q,t)\right\}dp\,dq, \tag{31}$$

respectively, and the magnetic resistivity and backscatter resistivity are given by

$$\xi_t(k|k_c;t)=-\frac{1}{k^2}\int\int_\triangle G(k)\frac{k}{pq}\theta_{kpq}(t)[h_{kpq}p^2E_v(q,t) + c_{kpq}k^2E_B(q,t)]dp\,dq, \tag{32}$$

$$\xi_b(k|k_c;t)=\frac{1}{2k^2\overline{E_B}(k,t)}\int\int_\triangle G(k)\theta_{kpq}(t) \times\frac{k^3}{pq}\left\{\frac{k^2}{p^2}c_{kpq}E_v(p,t)E_B(q,t) + h_{kpq}E_B(p,t)E_v(q,t)\right\}dp\,dq, \tag{33}$$

respectively.

To identify the terms that contribute to the eddy damping and backscatter, the resolved-scale MHD equations are written as

$$\left\{\frac{\partial}{\partial t}+[\nu+\nu_t(k|k_c;t)]k^2\right\}\overline{v_i}(\mathbf{k},t) = f_i^v(\mathbf{k},t)+M_{ijk}(\mathbf{k})\sum_\triangle G(k) \times[v_j(\mathbf{p},t)v_k(\mathbf{q},t)-B_j(\mathbf{p},t)B_k(\mathbf{q},t)] \tag{34}$$

and

$$\left\{\frac{\partial}{\partial t}+[\xi+\xi_t(k|k_c;t)]k^2\right\}\overline{B_i}(k,t) = f_i^b(\mathbf{k},t)+M_{ijk}^B(\mathbf{k})\sum_\triangle G(k)B_j(\mathbf{p},t)v_k(\mathbf{q},t). \tag{35}$$

The correlations of the stochastic backscatter forces, f_i^u and f_i^b, are $2k^2\overline{E_v}(k,t)\nu_b(k|k_c;t)$ and $2k^2\overline{E_B}(k,t)\xi_b(k|k_c;t)$, respectively.

IV. NUMERICAL RESULTS

Computations are performed for stationary, assumed spectra [21–25]

$$E_B(k)=\mathrm{Ko}\left(\frac{k}{k_p}\right)^{s+5/3}\frac{\epsilon^{2/3}k^{-5/3}}{1+\left(\frac{k}{k_p}\right)^{s+5/3}}, \tag{36}$$

$$E_v(k)=r_AE_B(k), \tag{37}$$

where $s=1$, $k_p=4$, and r_A is the Alfvén ratio. The assumed value of the Kolmogorov constant Ko is 1.7, and the energy dissipation rate ϵ is 7.24×10^4. The kinematic viscosity and magnetic resistivity are chosen as $\nu=\xi=0.004$. The wave number range is $k\in[1,512]$, with the discrete wave numbers

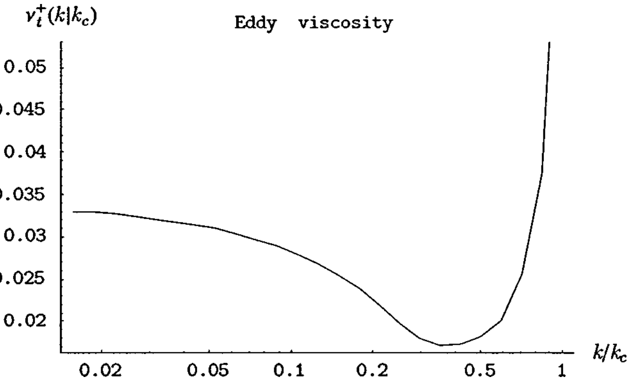

FIG. 1. The eddy viscosity (38) normalized according to Eq. (40) for the pure Navier-Stokes case.

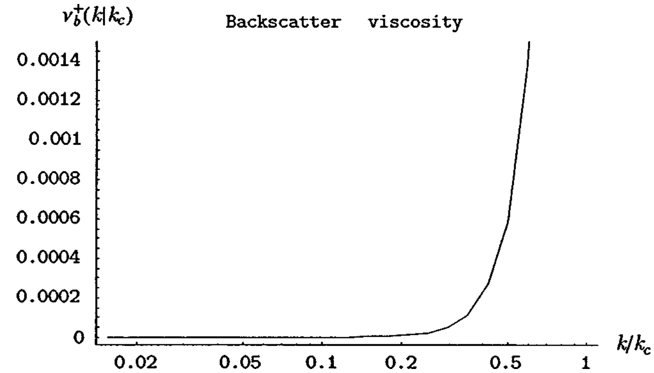

FIG. 2. The backscatter viscosity (39) normalized according to Eq. (41) for the pure Navier-Stokes case.

given by $k_l = k_{\min} 2^{(l-1)/4}$ with $k_{\min} = 1.0$ and $l = 1,...,37$. The cutoff wave number is taken to be $k_c = k_{\max}/8 = 64$.

Figures 1 and 2 show the eddy viscosity and backscatter viscosity for the pure Navier-Stokes case [25] given by

$$\nu_t(k|k_c;t) = \frac{1}{k^2} \int \int_{\triangle} G(k)\, \theta_{kpq}(t) \frac{kp}{q} b_{kpq} E_v(q,t)\, dp\, dq, \tag{38}$$

$$\nu_b(k|k_c;t) = \frac{1}{2k^2 \overline{E}_v(k,t)} \int \int_{\triangle} G(k)\, \theta_{kpq}(t) \times \frac{k^3}{pq} b_{kpq} E_v(p,t) E_v(q,t)\, dp\, dq, \tag{39}$$

respectively. The normalization is given by [17]

$$\nu_t(k|k_c;t) = \nu_t^+(k|k_c;t) \left[\frac{\overline{E}_v(k_c,t)}{k_c} \right]^{1/2}, \tag{40}$$

$$\nu_b(k|k_c;t) = \nu_b^+(k|k_c;t) \left[\frac{\overline{E}_v(k_c,t)}{k_c} \right]^{1/2}. \tag{41}$$

Figures 3 and 4 show the eddy viscosity and resistivity, and the backscatter viscosity and resistivity, respectively, for the nonhelical MHD case having $r_A = 1$, with the normalizations (40), (41), and

$$\xi_t(k|k_c;t) = \xi_t^+(k|k_c;t) \left[\frac{\overline{E}_B(k_c,t)}{k_c} \right]^{1/2}, \tag{42}$$

$$\xi_b(k|k_c;t) = \xi_b^+(k|k_c;t) \left[\frac{\overline{E}_B(k_c,t)}{k_c} \right]^{1/2}. \tag{43}$$

The addition of the magnetic field modifies the eddy and backscatter viscosities as follows. The eddy viscosity is slightly increased in magnitude due to the additional contribution of the magnetic term $1/k^2 \int\int_{\triangle} G(k)\, \theta_{kpq}(t) \times (kp/q) c_{kpq} E_B(q,t)\, dp\, dq$: this contribution increases in magnitude as $E_B(q,t)$ increases. The backscatter viscosity is also slightly increased in magnitude due to the additional contribution of the magnetic term $1/2k^2 \int\int_{\triangle} G(k)\, \theta_{kpq}(t) \times (kp/q) c_{kpq} E_B(q,t)\, dp\, dq$: this contribution also increases in magnitude as $E_B(q,t)$ increases. The eddy viscosity and eddy resistivity are comparable in magnitude and wave number dependence, with $\nu_t^+(k|k_c;t)$ somewhat larger than $\xi_t^+(k|k_c;t)$, particularly over the range $k/k_c \approx 0.3$–0.8. The backscatter viscosity and backscatter resistivity are also comparable in magnitude, with $\nu_b^+(k|k_c;t)$ slightly larger than $\xi_b^+(k|k_c;t)$ over all k/k_c.

For comparison, Figs. 5 and 6 show the eddy viscosity and resistivity, and the backscatter viscosity and resistivity, respectively, for the nonhelical MHD case having $r_A = \frac{1}{2}$, with the normalizations (40)–(43). The eddy resistivity and backscatter resistivity have a dependence on k/k_c, which is qualitatively very similar to that of the eddy viscosity and backscatter viscosity. The choice $r_A = \frac{1}{2}$ is motivated by solar wind observations [13,14]. The behaviors of these eddy and backscatter viscosities and resistivities are similar to that of the $r_A = 1$ case, except that both the eddy viscosity and backscatter viscosity have increased, while the eddy resistivity and backscatter resistivity have decreased significantly. Both $\xi_t^+(k|k_c;t)$ and $\xi_b^+(k|k_c;t)$ exhibit values near zero for a significant range of k/k_c.

V. CONCLUSIONS

The spectral eddy viscosity and resistivity, and backscatter viscosity and resistivity were computed for three-dimensional, incompressible, isotropic, nonhelical MHD turbulence using the EDQNM closure in terms of primitive fields **v** and **B**. Formal expressions for the eddy damping and backscatter terms in the resolved-scale velocity and magnetic field equations were presented using a straightforward application of the formalism used for Navier-Stokes turbulence by Leslie and Quarini [9] (see Ref. [25] for another recent application). The kinetic and magnetic energy spectra both had a production subrange and an inertial subrange, and were constructed for the two cases $r_A = 1$ and $r_A = \frac{1}{2}$. A numerical evaluation of these viscosities and resistivities showed that the addition of a magnetic field *increases* both the eddy and

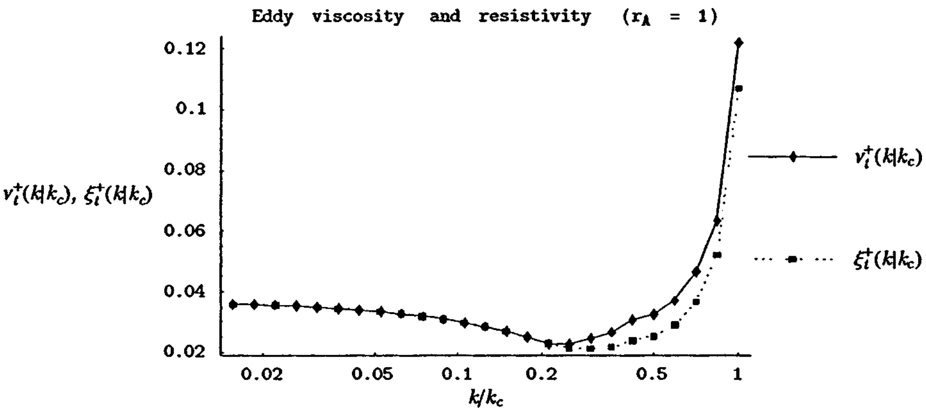

FIG. 3. The eddy viscosity (30) and eddy resistivity (32) normalized according to Eqs. (40) and (42), respectively, for the $r_A = 1$ case.

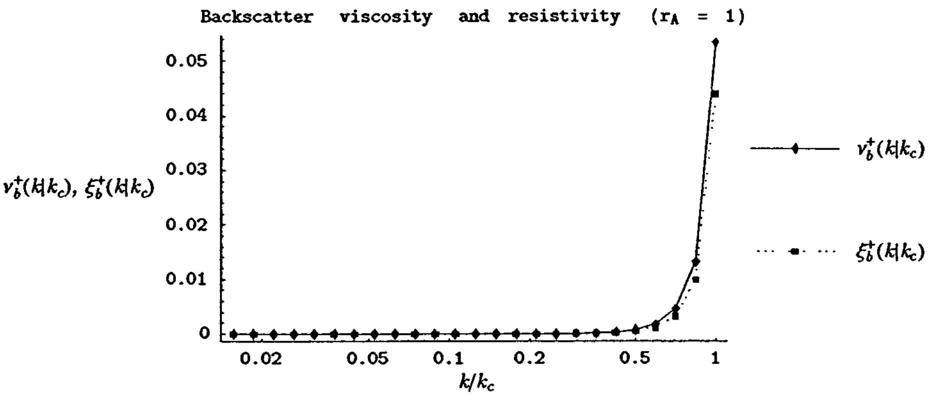

FIG. 4. The backscatter viscosity (31) and backscatter resistivity (33) normalized according to Eqs. (41) and (43), respectively, for the $r_A = 1$ case.

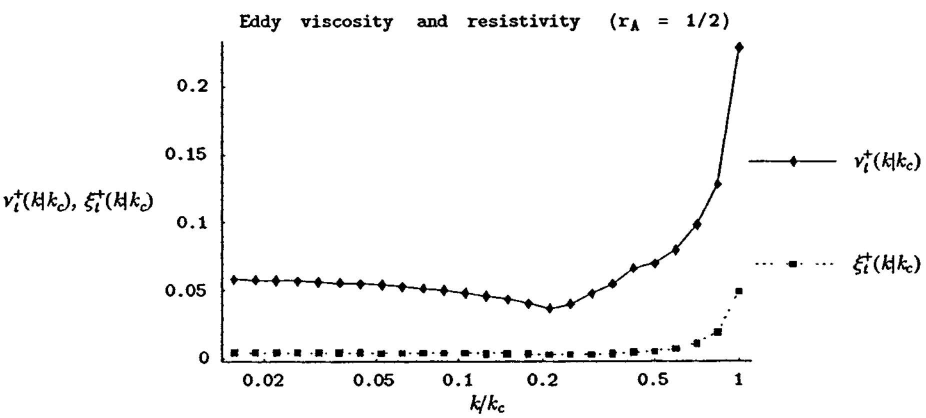

FIG. 5. The eddy viscosity (30) and eddy resistivity (32) normalized according to Eqs. (40) and (42), respectively, for the $r_A = \frac{1}{2}$ case.

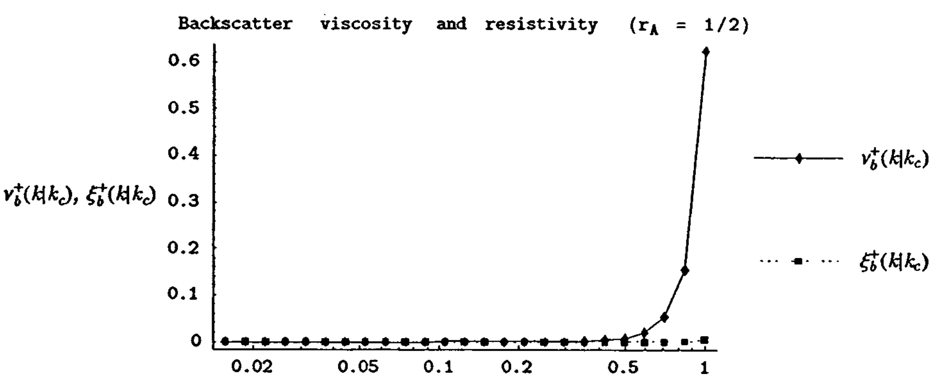

FIG. 6. The backscatter viscosity (31) and backscatter resistivity (33) normalized according to Eqs. (41) and (43), respectively, for the $r_A = \frac{1}{2}$ case.

backscatter viscosities. Also, the qualitative form and wave number dependence of the eddy and backscatter resistivities are similar to the eddy and backscatter viscosities. It is also apparent that the reduction of the Alfvén ratio results in smaller eddy resistivity and backscatter resistivity. The methodology developed here provides a statistical representation of the effects of the subgrid scales on the resolved scales, and has potential applications in spectral LES of large fluid and magnetic Reynolds number homogeneous MHD turbulence.

ACKNOWLEDGMENTS

This work was performed under the auspices of the U.S. Department of Energy by the University of California, Lawrence Livermore National Laboratory under Contract No. W-7405-Eng-48. This research was also supported by the National Science Foundation under Grant No. ATM 0096424. The calculations and plots were performed using MATHEMATICA® 4.1.

[1] A. Leonard, Adv. Geophys. **18**, 237 (1974).
[2] M. Lesieur and O. Metais, Annu. Rev. Fluid Mech. **28**, 45 (1996).
[3] *Large Eddy Simulation of Complex Engineering and Geophysical Flows*, edited by B. Galperin and S. A. Orszag (Cambridge University Press, Cambridge, 1993).
[4] D. R. Nicholson, *Introduction to Plasma Theory* (Wiley, New York, 1983).
[5] D. Biskamp, *Nonlinear Magnetohydrodynamics* (Cambridge University Press, Cambridge, 1997).
[6] Y. Zhou and G. Vahala, J. Plasma Phys. **45**, 239 (1991).
[7] A. Yoshizawa, J. Phys. Soc. Jpn. **60**, 9 (1991).
[8] M. L. Theobald, P. A. Fox, and S. Sofia, Phys. Plasmas **1**, 3016 (1994).
[9] D. C. Leslie and G. L. Quarini, J. Fluid Mech. **91**, 65 (1979).
[10] Y. Zhou, Phys. Rev. A **43**, 7049 (1991).
[11] W. H. Matthaeus and Y. Zhou, in *Turbulence and Nonlinear Dynamics in MHD Flows*, edited by M. Meneguzzi, A. Pouquet, and P. L. Sulem (Elsevier, Amsterdam, 1989).
[12] Y. Zhou and W. H. Matthaeus, J. Geophys. Res., [Space Phys.] **96**, 10 291 (1990).
[13] C.-Y. Tu and E. Marsch, *MHD Structures, Waves, and Turbulence in Solar Wind: Observations and Theories* (Kluwer Academic, Dordrecht, 1995).
[14] M. Goldstein, D. A. Roberts, and W. H. Mattheaus, Annu. Rev. Astron. Astrophys. **33**, 283 (1995).
[15] R. H. Kraichnan, J. Atmos. Sci. **33**, 1521 (1976).
[16] Y. Zhou and G. Vahala, Phys. Rev. E **47**, 2503 (1993).
[17] J.-P. Chollet and M. Lesieur, J. Atmos. Sci. **38**, 2747 (1981).
[18] R. Grappin, A. Pouquet, and J. Léorat, Astron. Astrophys. **126**, 51 (1983).
[19] J. Léorat, A. Pouquet, and U. Frisch, J. Fluid Mech. **104**, 419 (1981).
[20] A. Pouquet, U. Frisch, and J. Léorat, J. Fluid Mech. **77**, 321 (1976).
[21] R. H. Kraichnan, Phys. Fluids **8**, 1385 (1965).
[22] D. Fyfe, D. Montgomery, and G. Joyce, J. Plasma Phys. **17**, 369 (1977).
[23] W. H. Matthaeus and Y. Zhou, Phys. Fluids B **1**, 1929 (1989).
[24] Y. Zhou and W. H. Matthaeus, J. Geophys. Res., [Space Phys.] **95**, 14 881 (1990).
[25] O. Schilling and Y. Zhou, Phys. Fluids **14**, 1244 (2002).